Robust Deterministic Policy Gradient for Disturbance Attenuation and Its Application to Quadrotor Control*

Taeho Lee[1] and Donghwan Lee[1]

Abstract—**Practical control systems pose significant challenges in identifying optimal control policies due to uncertainties in the system model and external disturbances. While H_∞ control techniques are commonly used to design robust controllers that mitigate the effects of disturbances, these methods often require complex and computationally intensive calculations. To address this issue, this paper proposes a reinforcement learning algorithm called Robust Deterministic Policy Gradient (RDPG), which formulates the H_∞ control problem as a two-player zero-sum dynamic game. In this formulation, one player (the user) aims to minimize the cost, while the other player (the adversary) seeks to maximize it. We then employ deterministic policy gradient (DPG) and its deep reinforcement learning counterpart to train a robust control policy with effective disturbance attenuation. In particular, for practical implementation, we introduce an algorithm called robust deep deterministic policy gradient (RDDPG), which employs a deep neural network architecture and integrates techniques from the twin-delayed deep deterministic policy gradient (TD3) to enhance stability and learning efficiency.**

To evaluate the proposed algorithm, we implement it on an unmanned aerial vehicle (UAV) tasked with following a predefined path in a disturbance-prone environment. The experimental results demonstrate that the proposed method outperforms other control approaches in terms of robustness against disturbances, enabling precise real-time tracking of moving targets even under severe disturbance conditions.

I. INTRODUCTION

In recent years, significant advancements have been made in deep reinforcement learning (DRL), which integrates deep learning and reinforcement learning (RL). The successes of DRL have been demonstrated across various domains, including games [12], [13] and control [5], [14], [15]. Among the various challenging domains, this paper focuses on dynamic system control problems with continuous state-action spaces.

Practical dynamic control systems pose significant challenges in identifying optimal control policies due to unstructured uncertainties in the system model and external disturbances. Current state-of-the-art DRL methods for continuous control tasks, such as deep deterministic policy gradient (DDPG) [5], twin delayed DDPG (TD3) [4], soft actor-critic (SAC) [2], and proximal policy optimization (PPO) [3], generally fail to address these issues effectively. For instance, a DRL agent trained in a specific real-world or simulated environment may struggle to maintain optimal performance when deployed in different environments where the patterns of external disturbances changed. Therefore, developing a DRL agent policy that is robust to unseen disturbances is crucial for ensuring reliability in real-world applications.

The main goal of this paper is to introduce the robust deterministic policy gradient (RDPG) algorithm, which enhances the robustness of the DPG algorithm by integrating the concept of the H_∞ control problem with a two-player zero-sum dynamic game framework.

The H_∞ control method is a robust control technique that designs an optimal controller to minimize the impact of disturbances on its performance. It is well-known that, under certain assumptions, the H_∞ control problem can be transformed into a two-player zero-sum dynamic game (or a minmax optimization problem), where the first player, or the controller, tries to minimize a specific cost, while the second player, or the adversary, attempts to maximize it [21]. The minmax optimization problem can be solved by the Hamilton–Jacobi–Isaacs (HJI) equation. If the system is linear with quadratic costs, the solution of HJI equation can be derived through a Riccati equation [22], [23]. However, if the system has nonlinearity or the cost is non-quadratic, the HJI equation is extremely difficult to solve directly. Therefore, some methods have tried to obtain the approximate solution of HJI equations including power series expansion-based method [6], locally linearized mode [7], online learning algorithm with neural nets [10], and relaxed policy iteration algorithm with bounded policy evaluation error [11]. However, these methods are still associated with a high computational cost.

In this paper, we present the so-called robust deterministic policy gradient (RDPG) algorithm, which improves the robustness of DPG algorithm from the two-player zero-sum dynamic game perspectives. In particular, we transform the H_∞ problem into a two-player zero-sum dynamic game between the user (controller) and the adversary that represents the disturbance. Then, we propose a version of deterministic policy gradient method to train both the user and adversary, where the user and adversary each learn their own policy to minimize and maximize the objective function, respectively. Consequently, the robust controller can determine the optimal control input, which is robust against disturbances. The proposed RDPG is then extended to a DDPG variant, called RDDPG (robust DDPG), which combines the idea of RDPG with TD3.

Additionally, we aim to develop a robust control strategy for quadrotors, a commonly used unmanned aerial vehicle

[1]Taeho Lee and Donghwan Lee are with the School of Electrical Engineering, Korea Advanced Institute of Science and Technology (KAIST), Daejeon 34141, South Korea. email: eho0228,donghwan@kaist.ac.kr

(UAV) across various applications. Ensuring robust quadrotor control is essential, particularly for tasks such as tracking moving targets or following predefined waypoints in dynamic environments. We demonstrate that the proposed RDDPG method effectively determines optimal control inputs in the presence of external disturbances. Furthermore, it outperforms other DRL-based control approaches by achieving lower cost under severe disturbance conditions.

In conclusion, the main contributions can be summarized as follows:

1) We propose the robust deterministic policy gradient (RDPG) algorithm, which effectively improves the robustness against external disturbances by solving the H_∞ problem through the dynamic game perspectives in combination with the actor-critic method.
2) Moreover, we develop a new DDPG algorithm, called RDDPG, which combines the concept of RDPG with TD3. Through numerical simulations of the quadrotor control problems, the effectiveness of RDDPG is demonstrated.
3) Through the developed method, we propose a robust tracking control design method for quadrotor applications. Comprehensive experimental results are given to demonstrate that the proposed approach significantly outperforms other state-of-the-art DRL approaches such as DDPG, PPG, SAC, and TD3.

II. RELATED WORKS

The H_∞ control methods are effective in designing robust controllers against disturbances and have demonstrated satisfactory performance in nonlinear dynamic systems [6]–[9]. However, these methods require precise model linearization and incur a high computational costs due to the need to solve HJI equations. To address this issue, alternative approaches leverage deep reinforcement learning (DRL) to determine the optimal control policy, which does not require solving the nonlinear HJI equation.

Until now, the two-player zero-sum game and H_∞ control frameworks have been applied to deep reinforcement learning (DRL) to enhance robustness under various scenarios. For instance, [18] developed a robust DRL approach to bridge the gap between different environments for quadcopter control tasks. In [24], the authors proposed a novel approach for robust locomotion control of quadruped robots against external disturbances. A robust adversarial reinforcement learning strategy was proposed in [19] to address modeling errors and discrepancies between training and testing conditions. Although their underlying philosophy is similar to ours, their approaches are significantly different. The method in [24] solves two separate constrained optimization problems based on the ideas in PPO. The DRL in [18] primarily considers model uncertainties rather than external disturbances and applies the so-called action robust RL in [20], which has environmental structures different from our setting. The authors in [19] propose more general alternating optimization procedures and do not consider deterministic policy gradient.

III. BACKGROUND

A. H_∞ Control

Let us consider the discrete time nonlinear system

$$
\begin{aligned}
x_{k+1} &= f(x_k, u_k, w_k, v_k) \\
y_k &= g(x_k, u_k, w_k)
\end{aligned}
\tag{1}
$$

Using the state-feedback controller $u = \pi(x)$, the system can be reduced to the autonomous closed-loop system

$$
\begin{aligned}
x_{k+1} &= f(x_k, \pi(x_k), w_k, v_k) \\
y_k &= g(x_k, \pi(x_k), w_k)
\end{aligned}
$$

Assume that the initial state x_0 is determined by $x_0 \sim \rho(\cdot)$, where ρ is the initial state distribution. Defining the stochastic processes $\mathbf{w}_{0:\infty} := (w_0, w_1, \dots)$ and $\mathbf{y}_{0:\infty} := (y_0, y_1, \dots)$, the system can be seen as a stochastic mapping from $\mathbf{w}_{0:\infty}$ to $\mathbf{y}_{0:\infty}$ as follows:

$$
\mathbf{y}_{0:\infty} \sim T_\pi(\cdot | \mathbf{w}_{0:\infty}).
$$

where T_π is the conditional probability of $\mathbf{y}_{0:\infty}$ given $\mathbf{w}_{0:\infty}$. Moreover, defining the L^2 norm for the general stochastic process $\mathbf{z}_{0:\infty} := (z_0, z_1, \dots)$ by

$$
||\mathbf{z}_{0:\infty}||_{L^2} := \sqrt{\sum_{k=0}^{\infty} \mathbb{E}[z_k^T z_k]},
$$

the H_∞ norm of the autonomous system is defined as

$$
||T_\pi||_\infty := \sup_{\mathbf{w}_{0:\infty} \neq 0} \frac{||\mathbf{y}_{0:\infty}||_{L^2}}{||\mathbf{w}_{0:\infty}||_{L^2}}
\tag{2}
$$

The goal of H_∞ control is to design a control policy π that minimizes the H_∞ norm of the system T_π. However, minimizing $||T_\pi||_\infty$ directly is often difficult in practical implementations. Instead, we typically aim to find an acceptable $\eta > 0$ and a controller satisfying $||T_\pi||_\infty \leq \eta$, which is called suboptimal H_∞ control problem. Then, the H_∞ control problem can be approximated to the problem of finding a controller π that satisfies the constraint

$$
||T_\pi||_\infty^2 = \sup_{\mathbf{w}_{0:\infty} \neq 0} \frac{||\mathbf{y}_{0:\infty}||_{L^2}^2}{||\mathbf{w}_{0:\infty}||_{L^2}^2} \leq \eta^2
\tag{3}
$$

Defining

$$
J^\pi := \sup_{\mathbf{w}_{0:\infty} \neq 0} \mathbb{E}\left[\sum_{k=0}^{\infty} (y_k^T y_k - \eta^2 w_k^T w_k) \middle| \pi \right]
$$

the problem can be equivalently written by finding a controller π satisfying $J^\pi \leq 0$. The problem can be solved by

$$
\pi^* := \arg\min_\pi J^\pi.
$$

B. Two-player zero-sum dynamic game perspective

According to [21], the suboptimal H_∞ control problem can be equivalently viewed as solving a zero-sum dynamic game under certain assumptions. In particular, we consider two decision making agents called the user and the adversary, respectively. They sequentially take control actions u_k (user) and w_k (adversary) to minimize and maximize cumulative discounted costs, respectively, of the form $\mathbb{E}\left[\sum_{k=0}^\infty \gamma^k c(x_k, u_k, w_k)\right]$, where $\gamma \in (0,1]$ is the discount factor, u_k is the control input of the first agent, and w_k is the control input of the second agent. The user's primary goal entails minimizing the costs, while the adversary strives to hinder the user's progress by maximizing the costs. There exist two categories of the two-player dynamic games, the alternating two-player dynamic game and simultaneous two-player dynamic game. In the alternating two-player dynamic game, two agents engaged in decision making take turns in selecting actions to maximize and minimize the cost, respectively. On the other hand, in the simultaneous two-player dynamic game, the two agents take actions simultaneously to maximize and minimize the cost. In this paper, we mainly focus on the simultaneous two-player dynamic game.

We consider the state-feedback deterministic control policy for each agent, defined as $\pi : \mathbb{R}^n \to \mathbb{R}^m$ and $\mu : \mathbb{R}^n \to \mathbb{R}^p$

$$u = \pi(x) \in \mathbb{R}^m, \quad w = \mu(x) \in \mathbb{R}^p, \quad x \in \mathbb{R}^n$$

The corresponding cost function is defined as

$$J^{\pi,\mu} := \mathbb{E}\left[\sum_{k=0}^\infty \gamma^k c(x_k, u_k, w_k)\Bigg| \pi, \mu\right] \quad (4)$$

The goal of the dynamic game is to find a saddle-point pair of equilibrium policies (π, μ) (if exists) for which

$$J^{\pi^*,\mu} \leq J^{\pi^*,\mu^*} \leq J^{\pi,\mu^*}, \quad \forall \pi \in \Pi, \quad \forall \mu \in M$$

where Π denotes the set of all admissible state-feedback policies for the user and M denotes the set of all admissible state-feedback policies for the adversary. The above relation equivalently means

$$\mu^* = \max_{\mu \in M} J^{\pi^*,\mu}, \quad \pi^* = \min_{\pi \in \Pi} J^{\pi,\mu^*}$$

By the min-max theorem, this also implies that

$$\max_{\mu \in M} \min_{\pi \in \Pi} J^{\pi,\mu} = \min_{\pi \in \Pi} \max_{\mu \in M} J^{\pi,\mu}$$

The optimal cost is now defined as

$$J^* := J^{\pi^*,\mu^*}$$

To show a connection between the dynamic game framework and the H_∞ control problem, let us consider the specific per-step cost function

$$c(x,u,w) = g(x,u,w)^T g(x,u,w) - \eta^2 w^T w$$

where $v \sim p(\cdot)$ and $\gamma = 1$. The corresponding cost function is then written as

$$J^{\pi,\mu} = \mathbb{E}\left[\sum_{k=0}^\infty (y_k^T y_k - \eta^2 w_k^T w_k)\Bigg| \pi, \mu\right]$$

The user's optimal policy is

$$\pi^* := \arg\min_{\pi \in \Pi}\max_{\mu \in M} J^{\pi,\mu}$$

which is structurally very similar to the policy with the H_∞ performance in the previous subsection. It is known that under some special conditions such as the linearity, the H_∞ suboptimal control policy and the saddle-point policy are equivalent when $J^* \leq 0$.

C. Bellman equations

Let us define the value function

$$V^{\pi,\mu}(x) := \mathbb{E}\left[\sum_{k=t}^\infty \gamma^k c(x_k, u_k, w_k)\Bigg| \pi, \mu, x_t = x\right]$$

so that the corresponding cost function is $J^{\pi,\mu} = \mathbb{E}[V^{\pi,\mu}(x)|x \sim \rho(\cdot)]$. We can also prove that the value function satisfies the Bellman equation

$$V^{\pi,\mu}(x) = c(x, \pi(x), \mu(x)) + \gamma\mathbb{E}[V^{\pi,\mu}(x')|\pi, \mu]$$

where x' implies the next state given the current state x and the action taken by (π, μ). Let us define the optimal value function as $V^* := V^{\pi^*,\mu^*}$. Then, the corresponding optimal Bellman equation can be obtained by replacing (π, μ) by (π^*, μ^*). Similarly, let us define the so-called Q-function by

$$Q^{\pi,\mu}(x,u,w)$$
$$:= \mathbb{E}\left[\sum_{k=t}^\infty \gamma^k c(x_k, u_k, w_k)\Bigg| x_t = z, u_t = u, w_t = w, \pi, \mu\right]$$

which satisfies the Q-Bellman equation

$$Q^{\pi,\mu}(x,u,w) = c(x,u,w) + \gamma\mathbb{E}[Q^{\pi,\mu}(x',u',w')|\pi, \mu]$$

where x' implies the next state given the current state x and action pair (u,w), u' means the next action of the user given x' and under π, and w' implies the next action of the adversary given x' and under μ. Defining the optimal Q-function $Q^* := Q^{\pi^*,\mu^*}$, one can easily prove the optimal Q-Bellman equation

$$Q^*(x,u,w) = c(x,u,w) + \gamma\mathbb{E}[Q^*(x',u',w')|\pi^*, \mu^*]$$

IV. PROPOSED METHOD

In this section, we will present the proposed method.

A. Robust deterministic policy gradient

To apply DPG to the two-player zero-sum dynamic games, we consider the parameterized deterministic control policies

$$u = \pi_\theta(x) \in \mathbb{R}^m, \quad w = \mu_\phi(x) \in \mathbb{R}^p, \quad x \in R^n$$

The saddle-point problem is then converted to

$$\theta^* := \arg\min_\theta \max_\phi J^{\pi_\theta, \mu_\phi}$$

which can be solved using the primal-dual iteration

$$\theta_{k+1} = \theta_k - \alpha_\theta \nabla_\theta J^{\pi_\theta, \mu_{\phi_k}}\big|_{\theta=\theta_k},$$
$$\phi_{k+1} = \phi_k + \alpha_\phi \nabla_\phi J^{\pi_{\theta_{k+1}}, \mu_\phi}\big|_{\phi=\phi_k}$$

where $\alpha_\theta > 0$ and $\alpha_\phi > 0$ are step-sizes. According to [1], the deterministic gradients can be obtained using the following theorem.

Theorem 1: The deterministic policy gradients for the user and adversary policies are given by

$$\nabla_\theta J^{\pi_\theta, \mu_\phi} = E\left[\nabla_\theta Q^{\pi, \mu_\phi}(s, \pi_\theta, \mu_\phi)\big|_{\pi=\pi_\theta}\bigg| s \sim \rho^{\pi_\theta, \mu_\phi}\right]$$

and

$$\nabla_\phi J^{\pi_\theta, \mu_\phi} = E\left[\nabla_\phi Q^{\pi_\theta, \mu}(s, \pi_\theta, \mu_\phi)\big|_{\mu=\mu_\phi}\bigg| s \sim \rho^{\pi_\theta, \mu_\phi}\right]$$

respectively.

The proof is a simple extension of the DPG theorem in [1], so it is omitted here. A reinforcement learning counterpart to DPG can be obtained by using the samples of the gradients. Next, we will consider the following per-step cost function:

$$c(x, u, w) = \tilde{c}(x, u, w) - \eta^2 w^T w$$

where $\tilde{c} : \mathbb{R}^n \times \mathbb{R}^m \times \mathbb{R}^p \times \mathbb{R}^n \to \mathbb{R}$ is the cost function for the user. Note that the cost function $\tilde{c}$ can be set arbitrarily and is more general than the quadratic cost in the H_∞ control problem. This is because the H_∞ control problem can be recovered by setting

$$\tilde{c}(x, u, w) = g(x, u, w, v)^T g(x, u, w, v)$$

In this way, we can consider the two-player zero-sum dynamic game as an extension of the usual reinforcement learning tasks by considering robustness against the adversarial disturbance.

Let us assume that we found some approximate solutions $\theta_\epsilon^*, \phi_\epsilon^*$ such that $J^{\pi_{\theta_\epsilon^*}, \mu_{\phi_\epsilon^*}} \leq 0$. Then, this implies that

$$\frac{\mathbb{E}\left[\sum\limits_{k=0}^{\infty} \gamma^k \tilde{c}(x_k, u_k, w_k)\bigg| \pi_{\theta_\epsilon^*}, \mu_{\phi_\epsilon^*}\right]}{\mathbb{E}\left[\sum\limits_{k=0}^{\infty} \gamma^k w_k^T w_k\bigg| \pi_{\theta_\epsilon^*}, \mu_{\phi_\epsilon^*}\right]} \leq \eta^2$$

B. Implementation based on TD3 (RDDPG)

To implement RDPG for practical high-dimensional tasks, we will apply the techniques from twin-delayed deep deterministic policy gradient (TD3) in [4], which is called robust deep deterministic policy gradient (RDDPG). In particular, we introduce the following networks:

1) The online actor network π_θ for the user and the online actor network μ_ϕ for the adversary
2) The corresponding target networks $\pi_{\theta'}, \mu_{\phi'}$ for the two actors
3) Two online critic networks $Q_{\psi_1}(x, u, w), Q_{\psi_2}(x, u, w)$
4) The corresponding target networks $Q_{\psi_1'}(x, u, w)$, $Q_{\psi_2'}(x, u, w)$

Now, following [4], the actor and critic networks are trained through the following procedures.

1) Critic update: The critic is trained by the gradient descent step to the loss

$$L_{\text{critic}}(\psi_i; B) := \frac{1}{|B|} \sum_{(x,u,w,c,x') \in B} (y - Q_{\psi_i}(x, u, w))^2,$$
$$i \in \{1, 2\}$$

where B is the mini-batch, $|B|$ is the size of the mini-batch, c is the cost incurred at the same time as the state x, and x' means the next state. Moreover, the target y is defined as

$$y = c + \gamma \max_{i \in \{1, 2\}} Q_{\psi_i'}(x', \tilde{u}, \tilde{w})$$

when x' is not the terminal state, and

$$y = c$$

when x' is the terminal state (in the episodic environments), where

$$\tilde{u} = \pi_{\theta'}(x') + \text{clip}(\epsilon_1, -c, c) \quad \epsilon_1 \sim \mathcal{N}(0, \sigma)$$
$$\tilde{w} = \mu_{\phi'}(x') + \text{clip}(\epsilon_2, -c, c) \ , \quad \epsilon_2 \sim \mathcal{N}(0, \sigma)$$

where ϵ_1, ϵ_2 are random noise vectors added in order to smooth out the target values, $\mathcal{N}(0, \sigma)$ implies the Gaussian distribution with zero mean and variance σ, and the clip function is added in order to guarantee the boundedness of the control inputs. The critic's online parameters ϕ_1, ϕ_2 are updated by the gradient descent step to minimize the loss

$$\psi_i \leftarrow \psi_i - \alpha_{\text{critic}} L_{\text{critic}}(\psi_i; B), \quad i \in \{1, 2\}$$

where α_{critic} is the step-size.

2) Actor update: The actor networks for the user and adversary are updated using the sampled deterministic policy gradient

$$\theta \leftarrow \theta - \alpha_{\text{actor}} \nabla_\theta L_{\text{actor}}(\theta, \phi; B)$$
$$\phi \leftarrow \phi + \beta_{\text{actor}} \nabla_\phi L_{\text{actor}}(\theta, \phi; B)$$

where α_{actor} and β_{actor} are the step-sizes, and

$$L_{\text{actor}}(\theta, \phi; B) = \frac{1}{|B|} \sum_{(x,u,w,r,x') \in B} Q_{\psi_1}(x, \pi_\theta(x), \mu_\phi(x))$$

Please note the opposite signs of the gradients for the user and adversary updates, which are due to their opposite roles.

3) Target parameters update: The target parameters are updated through the averaging

$$\phi' \leftarrow \tau\phi + (1 - \tau)\phi', \quad \theta' \leftarrow \tau\theta + (1 - \tau)\theta'$$

for the actor target parameters and

$$\psi_i' \leftarrow \tau\psi_i + (1 - \tau)\psi_i', \quad i \in \{1, 2\}$$

for the critic target parameters.

4) Exploration: For exploration, we can use

$$u_k = \pi_\theta(x_k) + e_1$$
$$w_k = \mu_\phi(x_k) + e_2$$

where $e_1, e_2 \sim \mathcal{N}(0, \sigma)$ are exploration noises [4].

5) Optimizing η: As an objective function estimate, we use the target y used above. In particular, we simply assume

$$J^{\pi_{\theta'},\mu_{\phi'}} \cong \hat{J} := \frac{1}{|B|} \sum_{(x,u,w,r,x')\in B} y$$

where the target y is defined as before. Then, we can apply

$$J \leftarrow (1-\alpha_J)J + \alpha_J \hat{J}$$
$$\eta \leftarrow \eta + \alpha_\eta J$$

where J is an estimate of the cost function J^{π_θ,μ_ϕ}. The basic idea of the update rule for η is as follows: if $J > 0$, then increase $\eta > 0$ so that $J \leq 0$; if $J < 0$, then decrease $\eta > 0$ so that $J \leq 0$. In this way, we can find an optimal η such that $J \leq 0$. The overall algorithm is summarized in Algorithm 1.

Algorithm 1 RDDPG

1: Initialize the online critic networks Q_{ψ_1}, Q_{ψ_2}
2: Initialize the actor networks π_θ, μ_ϕ for the user and adversary, respectively.
3: Initialize the target parameters $\psi_1' \leftarrow \psi_1, \psi_2' \leftarrow \psi_2, \theta' \leftarrow \theta, \phi' \leftarrow \phi$
4: Initialize the replay buffer $\mathcal{D}$
5: **for** Episode $i=1,2,...N_{iter}$ **do**
6:     Observe s_0
7:     **for** Time step $k=0,1,2,...\tau$-1 **do**
8:         Select actions $u_k = \pi_\theta(x_k) + e_1$ and $w_k = \mu_\phi(x_k) + e_2$, where $e_1, e_2 \sim \mathcal{N}(0,\sigma)$ are exploration noises.
9:         Compute the cost $c_k := c(x_k, u_k, w_k)$
10:         Observe the next state x_{k+1}
11:         Store the transition tuple $(x_k, u_k, w_k, c_k, x_{k+1})$ in the replay buffer D
12:         Uniformly sample a mini-batch B from the replay buffer $\mathcal{D}$
13:         Update critic network:

$$\psi_i \leftarrow \psi_i - \alpha_{\text{critic}} L_{\text{critic}}(\psi_i; B), \quad i \in \{1,2\}$$

14:         Update actor networks by the deterministic policy gradient:

$$\theta \leftarrow \theta - \alpha_{\text{actor}} \nabla_\theta L_{\text{actor}}(\theta, \phi; B)$$
$$\phi \leftarrow \phi + \beta_{\text{actor}} \nabla_\phi L_{\text{actor}}(\theta, \phi; B)$$

15:         Update J and η:

$$J \leftarrow (1-\alpha_J)J + \alpha_J \hat{J}$$
$$\eta \leftarrow \eta + \alpha_\eta J$$

16:         Soft update target networks:
17:         $\theta_i' \leftarrow \tau\theta_i + (1-\tau)\theta_i'$, $\phi_i' \leftarrow \tau\theta_i + (1-\tau)\phi_i'$
18:     **end for**
19: **end for**

V. QUADROTOR APPLICATION

A. Quadrotor dynamics model

The quadrotor dynamics can be described as follows:

$$m\mathbf{a}_k = m \begin{bmatrix} 0 \\ 0 \\ -g \end{bmatrix} + \mathbf{RT}_k + \mathbf{F}_D + w_k \quad (5)$$

$$\Delta\omega_k = I^{-1}(-\omega_{k-1} \times I\omega_{k-1} + \tau_B) \quad (6)$$

$$\mathbf{v}_k = \mathbf{v}_{k-1} + T_s\mathbf{a}_k \quad (7)$$

$$\mathbf{p}_k = \mathbf{p}_{k-1} + T_s\mathbf{v}_k \quad (8)$$

$$\omega_k = \omega_{k-1} + T_s\Delta\omega_k \quad (9)$$

$$\rho_k = \rho_{k-1} + T_s\omega_k \quad (10)$$

where m is the mass of the quadrotor, g is the gravity acceleration, T_s is the sampling time, $w_k = [w_{k,x}, w_{k,y}, w_{k,z}]^T$ means an external disturbance applied to the quadrotor, $\mathbf{a}_k = [a_{k,x}, a_{k,y}, a_{k,z}]^T$ denotes linear acceleration, $\mathbf{v}_k = [v_{k,x}, v_{k,y}, v_{k,z}]^T$ represents linear velocity, $\mathbf{p}_k = [p_{k,x}, p_{k,y}, p_{k,z}]^T$ describes the position of the quadrotor in the inertial frame, $\Delta\omega_k = [\Delta\omega_{k,\phi}, \Delta\omega_{k,\theta}, \Delta\omega_{k,\psi}]^T$ is angular acceleration, $\omega_k = [\omega_{k,\phi}, \omega_{k,\theta}, \omega_{k,\psi}]^T$ is the angular velocity, and $\rho_k = [\phi_k, \theta_k, \psi_k]^T$ represents the roll, pitch, yaw of the quadrotor in the body frame. Moreover, $\mathbf{R}$ is the rotation matrix from the body frame to the inertial frame. Moreover, $\mathbf{T}_B$ is the total thrust of the quadrotor along the z axis in the body frame and defined as follows:

$$\mathbf{T}_k = \sum_{i=1}^4 T_{k,i} = k_F \begin{bmatrix} 0 \\ 0 \\ \sum \text{RPM}_{k,i}^2 \end{bmatrix}$$

where $T_{k,i}$ is the thrust generated by ith motor, k_F is the thrust coefficient, and $\text{RPM}_{k,i}$ is the speed of ith motor at time step k. $\mathbf{F}_D$ is a drag force, which is generated by motor spinning, defined as

$$\mathbf{F}_D = -\mathbf{K}_D \left(\sum_{i=1}^4 \text{RPM}_{k,i} \right) \mathbf{v}_k$$

where $\mathbf{K}_D = \text{diag}(K_{D,x}, K_{D,y}, K_{D,z})$ is a matrix of drag coefficients. Among the four motors, two opposing motors (1th and 3rd) rotate clockwise, while the others (2nd and 4th) rotate counterclockwise. This causes torque τ_k in the roll, pitch, yaw directions

$$\tau_k = \begin{bmatrix} \tau_{k,\phi} \\ \tau_{k,\theta} \\ \tau_{k,\psi} \end{bmatrix}$$
$$= \begin{bmatrix} l'k_F(\text{RPM}_{k,2}^2 - \text{RPM}_{k,4}^2) \\ l'k_F(-\text{RPM}_{k,1}^2 + \text{RPM}_{k,3}^2) \\ k_M(\text{RPM}_{k,1}^2 - \text{RPM}_{k,2}^2 + \text{RPM}_{k,3}^2 - \text{RPM}_{k,4}^2) \end{bmatrix}$$

where $l' = \cos(\frac{\pi}{4})l$ is the scaled arm length, because the motors of the quadrotor are positioned at a 45-degree angle relative to the x and y axes when the yaw angle is 0, k_F is the thrust coefficient, and k_M is the torque coefficient. The inertia matrix, denoted by the symbol I, represents the inertial properties of the quadrotor's body.

B. State space

The state x_k of the quadrotor is defined as

$$x_k = [\mathbf{e}_k^{\text{pos}}, \mathbf{e}_k^{\text{vel}}, \rho_k, \omega_k]^T \in \mathbb{R}^{12}$$

where

$$\mathbf{e}_k^{\text{pos}} = \mathbf{p}_k^{\text{target}} - \mathbf{p}_k$$
$$= [p_{k,x}^{\text{target}} - p_{k,x}, \; p_{k,y}^{\text{target}} - p_{k,y}, \; p_{k,z}^{\text{target}} - p_{k,z}]^T \in \mathbb{R}^3$$
$$\mathbf{e}_k^{\text{vel}} = \mathbf{v}_k^{\text{target}} - \mathbf{v}_k$$
$$= [v_{k,x}^{\text{target}} - v_{k,x}, \; v_{k,y}^{\text{target}} - v_{k,y}, \; v_{k,z}^{\text{target}} - v_{k,z}]^T \in \mathbb{R}^3$$
$$\rho_k = [\phi_k, \theta_k, \psi_k]^T \in \mathbb{R}^3$$
$$\omega_k = [\omega_{k,\phi}, \omega_{k,\theta}, \omega_{k,\psi}]^T \in \mathbb{R}^3$$

where $\mathbf{e}_k^{\text{pos}}$ is the position error between the target $\mathbf{p}_k^{\text{target}}$ and the quadrotor position $\mathbf{p}_k$, $\mathbf{e}_k^{\text{vel}}$ is the velocity error between the target $\mathbf{v}_k^{\text{target}}$ and the quadrotor $\mathbf{v}_k$, ρ_k is the Euler angle vector, and ω represents the angular velocity vector of the quadrotor in its body frame. As in the method used in DQN [13], we used the last four time steps of the state as input to the neural network to help the network better capture dynamics in the environment.

C. Action space

The action of the quadrotor, u_k, is the speed of four motors $\text{RPM}_{k,i}, i \in \{1, 2, 3, 4\}$, which is continuous value between 0 and 21713.714, as follows:

$$u_k := [\text{RPM}_{k,1}, \text{RPM}_{k,2}, \text{RPM}_{k,3}, \text{RPM}_{k,4}]^T \in \mathbb{R}^4.$$

The action of the disturbance adversary, w_k, represents the external forces to the quadrotor along the x, y, and z axes of the body frame as follows:

$$w_k := [w_{k,x}, w_{k,y}, w_{k,z}]^T \in \mathbb{R}^3$$

D. Cost function

The cost function $c(x_k, u_k, w_k)$ is comprised of the cost function for the user $\tilde{c}(x_k, u_k)$ and the disturbance quadratic cost $\eta^2 w_k^T w_k$. The cost function for the user $\tilde{c}(x_k, u_k)$ is the sum of the following terms: $\tilde{c}(x_k, u_k) = c_{k,p} + c_{k,v} + c_{k,\rho} + c_l + c_{tr}$

1) Position error cost $c_{k,p}$: Position error between the target and quadrotor

$$c_{k,p} = \alpha \times ||\mathbf{e}_k^{\text{pos}}||_2^2$$

2) Velocity error cost $c_{k,v}$: Velocity error between the target and quadrotor

$$c_{k,v} = \beta \times ||\mathbf{e}_k^{\text{vel}}||_2^2$$

3) Angle cost $c_{k,\rho}$: Magnitude of roll, pitch, and yaw of the quadrotor

$$c_{k,\rho} = \epsilon \times ||\rho_k||_2^2$$

4) Living cost c_l : Constant cost at every step

$$c_l = \lambda$$

5) Penalty cost c_{tr} : Penalty when the quadrotor fails to track the target

$$c_{tr} = \begin{cases} \zeta & \text{if } ||\mathbf{e}_k^{\text{pos}}||_2 \geq 5 \text{ or } \phi_k, \theta_k \geq \frac{\pi}{2} \\ 0 & \text{else} \end{cases}$$

where α, β, ϵ, $\zeta > 0$, and $\lambda < 0$ are scaling factors. Since α and β are positive, the agent learns a policy that minimizes position and velocity errors. If the quadrotor's angles become too large, it becomes more susceptible to disturbances and may flip easily. Therefore, minimizing the angles cost c_ρ is crucial for stability. Additionally, the living cost c_l is a negative reward that encourages the quadrotor to maintain stability. The penalty cost c_{tr} is a large positive value applied when the quadrotor fails to track the target—specifically, when the distance between the target and the quadrotor exceeds 5 meters, or when the quadrotor flips with roll or pitch angles exceeding $\frac{\pi}{2}$. The agent learns a policy to avoid receiving this penalty, which can accelerate the initial learning process.

VI. EXPERIMENTS AND RESULTS

A. Experiments setups

For experiments, we used gym-pybullet-drones environment [17], which is an open-source quadrotor simulator, built using Python and the Bullet Physics engine. This environment provides a modular and precise physics implementation, supporting both low-level and high-level controls. Crazyflie 2.0 quadrotor is modeled in the simulator, which is used for our experiments. In experiment, we compare RDDPG with DDPG [5], TD3 [4], SAC [2], and PPO [3]. These methods utilize a single agent aiming to minimize the cost function $\tilde{c}$. To enhance their robustness against disturbances, random external disturbances were applied during the learning process. From our own experiences, learning under severe disturbances with the four existing methods failed to yield policies that demonstrated reasonable performance. Therefore, we applied only minor disturbances, limited to ± 5 [m/s] when applying the four methods.

For evaluation, we generate three trajectories as shown in Fig. 1. During evaluation, we introduce random wind disturbances in the x and y directions of the inertia frame. We consider four scenarios where the maximum wind velocity is limited to ± 5, ± 10, ± 15, and ± 20 [m/s], which are referred to as the ± 5, ± 10, ± 15, and ± 20 wind speed scenarios in the tables. In each scenario, the initial wind speed is randomly set within a given range and updated every 10 time steps
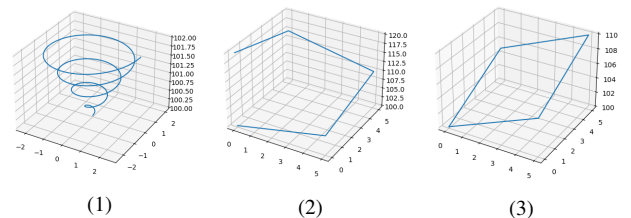

Fig. 1. Trajectories for evaluation.

TABLE I
The mean and standard deviation of the cost

Bold indicates the best performance algorithm

Algorithm	Trajectory		
	(1)	(2)	(3)
±5 wind speed scenario			
RDDPG	**−9.20 ± 0.03**	**−9.11 ± 0.02**	**−8.94 ± 0.03**
DDPG	−7.63 ± 0.09	−7.67 ± 0.10	−7.49 ± 0.12
TD3	−4.25 ± 2.47	−7.50 ± 1.65	−6.00 ± 2.53
SAC	−7.42 ± 0.98	−8.68 ± 0.26	−8.34 ± 0.30
PPO	19.26 ± 12.01	7.72 ± 8.37	11.03 ± 9.54
±10 wind speed scenario			
RDDPG	**−9.00 ± 0.12**	**−8.96 ± 0.16**	**−8.73 ± 0.21**
DDPG	−7.41 ± 0.24	−7.41 ± 0.28	−7.20 ± 0.43
TD3	0.45 ± 5.95	−2.20 ± 5.00	−0.94 ± 5.00
SAC	−7.16 ± 1.05	−7.94 ± 0.71	−7.54 ± 0.87
PPO	22.89 ± 15.31	22.22 ± 15.42	22.71 ± 15.64
±15 wind speed scenario			
RDDPG	**−8.49 ± 0.52**	**−8.36 ± 0.71**	**−8.17 ± 0.62**
DDPG	−5.95 ± 2.03	−5.98 ± 1.90	−5.76 ± 1.78
TD3	3.02 ± 6.49	1.90 ± 6.28	2.64 ± 5.45
SAC	−2.86 ± 4.55	−3.70 ± 4.03	−3.32 ± 4.13
PPO	23.63 ± 17.10	23.45 ± 16.95	23.27 ± 15.77
±20 wind speed scenario			
RDDPG	**−5.04 ± 3.90**	**−4.77 ± 4.07**	**−4.46 ± 4.03**
DDPG	0.18 ± 5.56	−0.04 ± 5.76	−0.51 ± 5.28
TD3	3.76 ± 5.32	3.27 ± 4.88	3.66 ± 4.77
SAC	0.18 ± 4.64	0.49 ± 4.96	0.61 ± 4.98
PPO	20.81 ± 15.58	21.15 ± 15.12	21.32 ± 16.77

TABLE II
Empirically evaluated H_∞ norm.

Bold indicates the best performance algorithm

Algorithm	Trajectory		
	(1)	(2)	(3)
±5 wind speed scenario			
RDDPG	**247.14**	**284.04**	**299.59**
DDPG	7874.49	570.36	999.50
TD3	1421.04	573.83	820.78
SAC	708.79	749.96	593.65
PPO	8360.81	4086.99	7548.96
±10 wind speed scenario			
RDDPG	**74.17**	**112.76**	**84.36**
DDPG	185.82	282.43	202.59
TD3	422.65	331.02	351.93
SAC	209.82	144.25	123.55
PPO	2314.39	4058.31	2308.93
±15 wind speed scenario			
RDDPG	**59.29**	**44.00**	**41.09**
DDPG	75.45	87.31	82.17
TD3	216.96	147.81	216.73
SAC	103.45	75.54	89.90
PPO	6286.04	1281.48	2862.71
±20 wind speed scenario			
RDDPG	**140.33**	**30.06**	**53.50**
DDPG	76.90	83.34	79.91
TD3	284.40	205.07	176.43
SAC	88.42	73.83	78.32
PPO	1278.23	885.98	1576.79

with normally distributed noise. Each algorithm was tested over 500 episodes and evaluated using three metrics: the mean and standard deviation of the total cost per episode, the average H_∞ norm, empirically evaluated as $\frac{\bar{c}(x_k, u_k, w_k)}{w_k^T w_k}$, and the mean and standard deviation of the position error between the quadrotor and the target. All metrics were averaged over 500 episodes.

B. Results

Fig. 2 shows the sum of costs during the training steps, demonstrating that RDDPG effectively minimizes the cost as training progresses
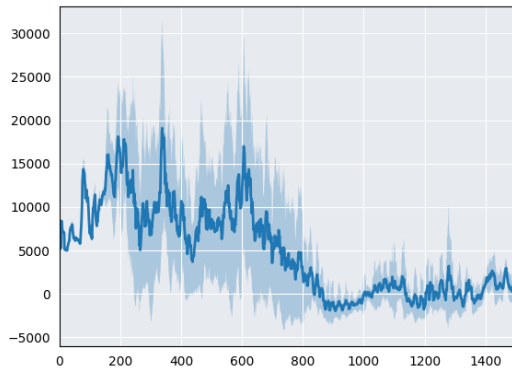

Fig. 2. The cost curve of RDDPG during training. This shows that RDDPG success to minimize the cost as training progresses.

Table I presents the mean and standard deviation of the total cost sum per episode. Across all scenarios, RDDPG achieved the lowest total cost sum, which demonstrates superior performance compared to other algorithms. Notably, TD3, the baseline algorithm for RDDPG, exhibited significant performance degradation as wind conditions intensified. In contrast, RDDPG maintained a lower cost sum and greater stability, indicating that RDPG enhances the robustness of the DPG algorithm.

Table II describes the mean of H_∞ norm at time step k in all wind speed scenarios. As the wind speed decreases, the magnitude of disturbances also diminishes. Since the H_∞ norm is inversely proportional to the disturbance magnitude, scenarios with weaker wind conditions tend to exhibit higher H_∞ norm values. RDDPG exhibits a smaller H_∞ norm than the other algorithms; this implies that RDDPG effectively minimizes the cost in disturbance scenarios

Table III presents the mean and standard deviation of the positional errors between the target and the quadrotor at time step k. DDPG performs best in low wind speed scenarios, RDDPG achieves lower errors as wind speed increases. Although DDPG exhibits smaller distance errors, its higher total cost in Table I suggests that the quadrotor experiences large angular deviations and significant oscillations. These oscillations make the DDPG controller more vulnerable to strong winds, ultimately causing instability in high-wind scenarios.

TABLE III

THE MEAN AND STANDARD DEVIATION OF THE POSITION ERROR $||e_k^{pos}||_2$ BETWEEN THE TARGET AND THE QUADROTOR

Bold indicates the best performance algorithm

Algorithm	Trajectory		
	(1)	(2)	(3)
±5 wind speed scenario			
RDDPG	0.17 ± 0.02	0.16 ± 0.02	0.17 ± 0.03
DDPG	$\mathbf{0.13 \pm 0.05}$	$\mathbf{0.12 \pm 0.05}$	$\mathbf{0.12 \pm 0.07}$
TD3	0.35 ± 0.28	0.21 ± 0.11	0.26 ± 0.17
SAC	0.27 ± 0.16	0.20 ± 0.07	0.22 ± 0.09
PPO	0.91 ± 0.65	0.86 ± 0.43	0.76 ± 0.51
±10 wind speed scenario			
RDDPG	0.18 ± 0.04	0.18 ± 0.03	0.19 ± 0.05
DDPG	$\mathbf{0.16 \pm 0.06}$	$\mathbf{0.15 \pm 0.07}$	$\mathbf{0.15 \pm 0.08}$
TD3	0.48 ± 0.39	0.38 ± 0.32	0.42 ± 0.33
SAC	0.29 ± 0.16	0.25 ± 0.11	0.27 ± 0.13
PPO	1.16 ± 0.82	1.13 ± 0.78	1.14 ± 0.77
±15 wind speed scenario			
RDDPG	$\mathbf{0.22 \pm 0.07}$	$\mathbf{0.21 \pm 0.07}$	$\mathbf{0.22 \pm 0.07}$
DDPG	0.23 ± 0.15	0.23 ± 0.15	0.23 ± 0.15
TD3	0.56 ± 0.42	0.52 ± 0.37	0.55 ± 0.40
SAC	0.46 ± 0.28	0.43 ± 0.26	0.43 ± 0.27
PPO	1.50 ± 1.16	1.50 ± 1.12	1.50 ± 1.14
±20 wind speed scenario			
RDDPG	$\mathbf{0.22 \pm 0.07}$	$\mathbf{0.21 \pm 0.07}$	$\mathbf{0.22 \pm 0.07}$
DDPG	0.37 ± 0.36	0.36 ± 0.36	0.35 ± 0.33
TD3	0.60 ± 0.47	0.57 ± 0.44	0.60 ± 0.46
SAC	0.51 ± 0.36	0.51 ± 0.37	0.51 ± 0.38
PPO	1.60 ± 1.28	1.57 ± 1.26	1.53 ± 1.20

VII. CONCLUSION

This paper proposes RDPG, which combines the concept of the H_∞ control problem and a two-player zero-sum dynamic game framework, to overcome the robustness problem of DRL algorithms. In RDPG, the user aims to minimize the cost function while the adversary tries to maximize it. Additionally, we introduce the RDDPG algorithm, which integrates RDPG with TD3 to improve both robustness and learning efficiency. In order to evaluate the robustness of RDDPG, we implement it on the tracking tasks of the quadrotor. Experimental results show that RDDPG can achieve the optimal control policy and maintain stability in various environments with disturbances. This demonstrates that RDDPG outperforms other DRL methods in terms of robustness.

REFERENCES

[1] Silver, D., Lever, G., Heess, N., Degris, T., Wierstra, D., and Riedmiller, M. (2014, January). Deterministic policy gradient algorithms. In International conference on machine learning (pp. 387-395). PMLR.

[2] Haarnoja, T., Zhou, A., Abbeel, P., and Levine, S. (2018, July). Soft actor-critic: Off-policy maximum entropy deep reinforcement learning with a stochastic actor. In International conference on machine learning (pp. 1861-1870). Pmlr.

[3] Schulman, J., Wolski, F., Dhariwal, P., Radford, A., and Klimov, O. (2017). Proximal policy optimization algorithms. arXiv preprint arXiv:1707.06347.

[4] Fujimoto, S., Hoof, H., and Meger, D. (2018, July). Addressing function approximation error in actor-critic methods. In International conference on machine learning (pp. 1587-1596). PMLR.

[5] Lillicrap, T. P. (2015). Continuous control with deep reinforcement learning. arXiv preprint arXiv:1509.02971.

[6] Huang, J., and Lin, C. F. (1995). Numerical approach to computing nonlinear H-infinity control laws. Journal of Guidance, Control, and Dynamics, 18(5), 989-994.

[7] Rigatos, G., Siano, P., Wira, P., and Profumo, F. (2015). Nonlinear H-infinity feedback control for asynchronous motors of electric trains. Intelligent Industrial Systems, 1, 85-98.

[8] Al-Tamimi, A., Lewis, F. L., and Abu-Khalaf, M. (2007). Model-free Q-learning designs for linear discrete-time zero-sum games with application to H-infinity control. Automatica, 43(3), 473-481.

[9] Le Ballois, S., and Duc, G. (1996). H-infinity control of an Earth observation satellite. Journal of guidance, control, and dynamics, 19(3), 628-635.

[10] Modares, Hamidreza, Frank L. Lewis, and Mohammad-Bagher Naghibi Sistani. Online solution of nonquadratic two-player zero-sum games arising in the H-infinity control of constrained input systems. International Journal of Adaptive Control and Signal Processing 28.3-5 (2014): 232-254.

[11] Li, Jie, et al. "Relaxed Policy Iteration Algorithm for Nonlinear Zero-Sum Games With Application to H-Infinity Control." IEEE Transactions on Automatic Control 69.1 (2023): 426-433.

[12] Silver, D., Schrittwieser, J., Simonyan, K., Antonoglou, I., Huang, A., Guez, A., ... and Hassabis, D. (2017). Mastering the game of go without human knowledge. nature, 550(7676), 354-359.

[13] Mnih, V., Kavukcuoglu, K., Silver, D., Rusu, A. A., Veness, J., Bellemare, M. G., ... and Hassabis, D. (2015). Human-level control through deep reinforcement learning. nature, 518(7540), 529-533.

[14] Kalashnikov, D., Irpan, A., Pastor, P., Ibarz, J., Herzog, A., Jang, E., ... and Levine, S. (2018, October). Scalable deep reinforcement learning for vision-based robotic manipulation. In Conference on robot learning (pp. 651-673). PMLR.

[15] Wang, S., Jia, D., and Weng, X. (2018). Deep reinforcement learning for autonomous driving. arXiv preprint arXiv:1811.11329.

[16] Yuste, P. C., Martínez, J. A. I., and de Miguel, M. A. S. (2024). Simulation-based evaluation of model-free reinforcement learning algorithms for quadcopter attitude control and trajectory tracking. Neurocomputing, 608, 128362.

[17] Panerati, J., Zheng, H., Zhou, S., Xu, J., Prorok, A., and Schoellig, A. P. (2021, September). Learning to fly—a gym environment with pybullet physics for reinforcement learning of multi-agent quadcopter control. In 2021 IEEE/RSJ International Conference on Intelligent Robots and Systems (IROS) (pp. 7512-7519). IEEE.

[18] Deshpande, A. M., Minai, A. A., and Kumar, M. (2021). Robust deep reinforcement learning for quadcopter control. IFAC-PapersOnLine, 54(20), 90-95.

[19] Pinto, L., Davidson, J., Sukthankar, R., and Gupta, A. (2017, July). Robust adversarial reinforcement learning. In International conference on machine learning (pp. 2817-2826). PMLR.

[20] Tessler, C., Efroni, Y., and Mannor, S. (2019, May). Action robust reinforcement learning and applications in continuous control. In International Conference on Machine Learning (pp. 6215-6224). PMLR.

[21] Başar, Tamer, and Pierre Bernhard. H-infinity optimal control and related minimax design problems: a dynamic game approach. Springer Science and Business Media, 2008.

[22] Basar, Tamer. "A dynamic games approach to controller design: Disturbance rejection in discrete time." Proceedings of the 28th IEEE Conference on Decision and Control,. IEEE, 1989.

[23] Stoorvogel, A. A., and Weeren, A. J. (1994). The discrete-time riccati equation related to the H_∞ control problem. IEEE Transactions on Automatic Control, 39(3), 686-691.

[24] Long, J., Yu, W., Li, Q., Wang, Z., Lin, D., and Pang, J. (2024). Learning H-Infinity Locomotion Control. arXiv preprint arXiv:2404.14405.